

## INVERSE THERMAL DESIGN OF THERMO-MAGNETICALLY DRIVEN BOUSSINESQ FLOWS

Rajiv Sampath and Nicholas Zabaras\*

Sibley School of Mechanical and Aerospace Engineering  
 188 Frank H.T. Rhodes Hall, Cornell University  
 Ithaca, NY 14853-3801  
 Email: zabaras@cornell.edu

### ABSTRACT

A methodology for the solution of an ill-posed inverse magneto-convection problem is proposed. In particular, an incompressible, viscous, electrically conducting liquid material occupying a domain  $\Omega$  is considered. Convection is driven by buoyancy effects and an applied magnetic field. Thermal boundary conditions are only prescribed in the part  $(\Gamma - \Gamma_{h0})$  of the boundary  $\Gamma$ . In addition, the temperature distribution is also prescribed in the part  $\Gamma_I$  of the boundary  $\Gamma_{h1}$  where the heat flux is known, i.e.  $\Gamma_I$  is a boundary with overspecified thermal boundary conditions. The inverse problem is posed as a functional optimization problem for the calculation of the boundary heat flux  $q_o(\mathbf{x}, t)$ , with  $(\mathbf{x}, t) \in (\Gamma_{h0} \times [0, t_{max}])$ . To account for random errors in the given temperature data, a  $H^1$  type regularization is introduced. The gradient of the cost functional is obtained from appropriately defined adjoint fields. The optimization algorithm is solved using the conjugate gradient method. The method is demonstrated through the solution of an inverse problem with known results. Finally, some potential applications are identified.

### NOMENCLATURE

English:

$\mathbf{B}_0$  Applied magnetic field  
 $c$  Specific heat  
 $\mathbf{e}_g$  Unit vector in the direction of gravity  
 $\mathbf{e}_B$  Unit vector in the direction of  $\mathbf{B}_0$   
 $\mathbf{E}$  Electric field intensity  $\equiv -\nabla\phi$

$Ha$  Hartmann number  $\equiv \left[ \left( \frac{\sigma_e}{\rho\nu} \right)^{1/2} B_0 L \right]$   
 $\mathbf{I}$  Unit second order tensor  
 $\mathbf{J}$  Electric current density  
 $J$  Cost functional  
 $J'$  Gradient of the cost functional  
 $k$  Conductivity  
 $L$  Length scale  
 $L_2$  Square integrable function space  
 $n_{sd}$  Space dimension (1, 2, 3)  
 $p$  Dimensionless pressure  
 $Pr$  Prandtl number  $\equiv \nu/\alpha$   
 $q$  Dimensionless heat flux  
 $\mathfrak{R}^{n_{sd}}$  Real vector space  
 $Ra$  Rayleigh number  $\equiv g\beta(T_{in} - T_{ref})L^3/\nu\alpha$   
 $t$  Dimensionless time  
 $T$  Actual temperature  
 $T_{in}$  Initial temperature  
 $T_{ref}$  Reference temperature  
 $\hat{\mathbf{v}}$  Fluid velocity vector  
 $\mathbf{v}$  Dimensionless fluid velocity vector  
 $\mathbf{V}$  The sensitivity velocity field  $\equiv D_{\Delta q_o} \mathbf{v}(\mathbf{x}, t; q_o)$   
 $\mathbf{x}$  Dimensionless spatial coordinates in  $\Omega$   
 Greek:  
 $\alpha$  Thermal diffusivity  $\equiv k/\rho c$   
 $\beta$  Thermal expansion coefficient  
 $\Gamma$  Boundary of the domain  $\Omega$   
 $\Gamma_g$  Dirichlet boundary of the domain  
 $\Gamma_h$  Neumann boundary of the domain

\*Address all correspondence to this author.

$\Gamma_{h0}$	Boundary with unknown heat flux
$\Gamma_{h1}$	Boundary with known heat flux
$\Gamma_I$	Boundary with prescribed temperature and heat flux
$\theta$	Dimensionless temperature $\equiv (T - T_{ref}) / (T_{in} - T_{ref})$
$\theta_m$	Prescribed temperature in $\Gamma_I$
$\Theta$	Sensitivity temperature field $\equiv D_{\Delta q_0} \theta(\mathbf{x}, t; q_0)$
$\eta$	Adjoint electric potential field
$\Pi$	Sensitivity pressure field $\equiv D_{\Delta q_0} p(\mathbf{x}, t; q_0)$
$\rho_e$	Electric charge density
$\sigma$	Dimensionless stress tensor
$\sigma_e$	Electrical conductivity
$\Sigma$	Sensitivity stress tensor $\equiv D_{\Delta q_0} \sigma(\mathbf{x}, t; q_0)$
$\pi$	Adjoint pressure
$\zeta$	Adjoint stress tensor
$\phi$	Adjoint velocity field
$\psi$	Adjoint temperature field
$\hat{\phi}$	Electric field potential
$\varphi$	Dimensionless electric field potential $\equiv \hat{\phi} / \alpha B_0$
$\Phi$	Sensitivity electric potential field $\equiv D_{\Delta q_0} \varphi(\mathbf{x}, t; q_0)$
$\Omega$	Domain
$\omega_n$	Uniformly distributed random numbers in $[-1, 1]$

## INTRODUCTION

Many design problems can be posed as inverse problems in which incomplete information is prescribed on one part of the boundary, whereas overspecified boundary conditions are supplied on another part of the boundary or inside the domain. These problems are ill-posed in the sense that their solution (if it exists) is unstable to perturbations in the given data [1;21;22]. Applications to convection problems can be found in [4;6;7;13;15;20;21;22].

In recent years, considerable research efforts have been directed towards the design of fluid flow systems in the presence of a magnetic field. Examples include the design of self-cooled liquid-metal blanket of a magnetically confined fusion reactor [9] and a number of applications in materials processing including electro-magnetic stirring of continuous castings and control of microstructures in semiconductor crystal growth [16;20]. In this paper, a free convecting, incompressible, electrically conducting, viscous fluid in the presence of a strong applied magnetic field is considered. The design problem of interest refers to the calculation of the heat flux in part of the boundary that results in a desired temperature distribution in another part of the boundary, where the heat flux is prescribed. This inverse problem is of relevance to many engineering systems involving fluid flow and heat transfer in a strong magnetic field (e.g. see [15] for an application to the design of solidification processes).

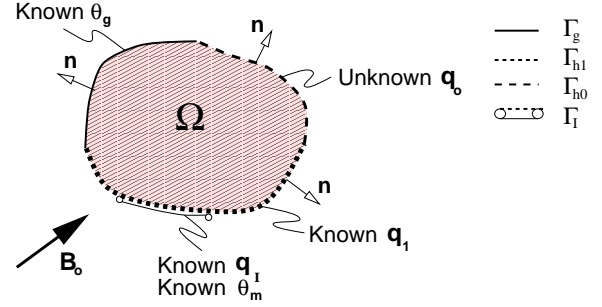


Figure 1. SCHEMATIC OF THE INVERSE MAGNETO-CONVECTION PROBLEM.

## FORMULATION

Let  $\Omega$  be a closed bounded region in  $\mathcal{R}^{n_{sd}}$ , with a piecewise smooth boundary  $\Gamma$  (Fig. 1). The region is occupied by an incompressible electrically conducting fluid and is subject to an external constant magnetic field  $\mathbf{B}_0$  in a non-isothermal environment. The motion of this fluid is initially driven by temperature induced density gradients. Motion in the presence of a magnetic field  $\mathbf{B}$  will give rise to a Lorentz force  $\mathbf{F}$  acting on the fluid:

$$\mathbf{F} = \rho_e \mathbf{E} + \mathbf{J} \times \mathbf{B} \quad (1)$$

The electric current density is governed by Ohm's law:

$$\mathbf{J} = \rho_e \hat{\mathbf{v}} + \sigma_e (-\nabla \hat{\phi} + \hat{\mathbf{v}} \times \mathbf{B}) \quad (2)$$

We assume that the walls of the cavity are electric insulators and that the induced magnetic field is negligible with respect to the imposed constant magnetic field  $\mathbf{B}_0$ . This condition generally holds good in liquid metal and semiconductor melts due to the small magnetic Reynolds number in these systems. We assume that the conducting fluid is approximately grossly neutral and hence the charge density  $\rho_e$  is actually the excess charge density, which is very small in liquid metal melts. Hence, the terms  $\rho_e \mathbf{E}$  and  $\rho_e \hat{\mathbf{v}}$  in Eqs. (1) and (2), respectively, are neglected [3;12]. The conservation of electric current  $\nabla \cdot \mathbf{J} = 0$  can then be used to eliminate  $\mathbf{J}$  and to write the governing equations in terms of  $\hat{\phi}$ . The governing equation for  $\hat{\phi}$  is as follows:

$$\nabla^2 \hat{\phi} = \nabla \cdot (\hat{\mathbf{v}} \times \mathbf{B}) \quad (3)$$

Thus, Eq. (3) gives the potential function and this function along with  $\mathbf{B}_0$  determines  $\mathbf{F}$  in Eq. (1). The resulting induced flow is modeled using the Navier-Stokes equations employing a Boussinesq approximation to handle density change due temperature variations in the fluid. Note that only dimensionless quantities will be used in the rest of this paper (see the Nomenclature for the definition of the various dimensionless quantities).

In the part  $\Gamma_h$  of the boundary  $\Gamma$ , we assume that a heat flux boundary condition is applied, whereas in the remaining part of the boundary,  $\Gamma_g$ , a temperature boundary condition is considered (Fig. 1). However, the distribution of the boundary heat flux on  $\Gamma_{h0} \subset \Gamma_h$  is not known ( $\Gamma_{h0} \cup \Gamma_{h1} = \Gamma_h$ ,  $\Gamma_{h0} \cap \Gamma_{h1} = \emptyset$ ). The known flux and temperature distributions are given below:

$$\theta(\mathbf{x}, t) = \theta_g(\mathbf{x}, t), \quad (\mathbf{x}, t) \in \Gamma_g \times [0, t_{max}], \quad (4)$$

$$q(\mathbf{x}, t) \equiv \nabla\theta(\mathbf{x}, t) \cdot \mathbf{n} = q_1(\mathbf{x}, t), \quad (\mathbf{x}, t) \in \Gamma_{h1} \times [0, t_{max}], \quad (5)$$

and the *unknown* flux distribution on  $\Gamma_{h0}$  is

$$q(\mathbf{x}, t) \equiv \nabla\theta(\mathbf{x}, t) \cdot \mathbf{n} = q_o(\mathbf{x}, t), \quad (\mathbf{x}, t) \in \Gamma_{h0} \times [0, t_{max}]. \quad (6)$$

### Box I

DIRECT PROBLEM TO DEFINE  $\theta(\mathbf{x}, t; q_o)$ ,  $\mathbf{v}(\mathbf{x}, t; q_o)$  AND  $\boldsymbol{\varphi}(\mathbf{x}, t; q_o)$

$$\frac{\partial\theta(\mathbf{x}, t)}{\partial t} + \mathbf{v}(\mathbf{x}, t) \cdot \nabla\theta(\mathbf{x}, t) = \nabla^2\theta(\mathbf{x}, t), \quad (\mathbf{x}, t) \in \Omega \times [0, t_{max}] \quad (7)$$

$$\begin{aligned} \frac{\partial\mathbf{v}(\mathbf{x}, t)}{\partial t} + (\nabla\mathbf{v}(\mathbf{x}, t))\mathbf{v}(\mathbf{x}, t) = \nabla \cdot \boldsymbol{\sigma}(\mathbf{x}, t) - RaPr\theta(\mathbf{x}, t)\mathbf{e}_g \\ + Ha^2Pr[-\nabla\boldsymbol{\varphi}(\mathbf{x}, t) + \mathbf{v}(\mathbf{x}, t) \times \mathbf{e}_B] \times \mathbf{e}_B, \quad (\mathbf{x}, t) \in \Omega \times [0, t_{max}] \quad (8) \end{aligned}$$

$$\boldsymbol{\sigma}(\mathbf{x}, t) = -p(\mathbf{x}, t)\mathbf{I} + Pr[\nabla\mathbf{v}(\mathbf{x}, t) + (\nabla\mathbf{v}(\mathbf{x}, t))^T], \quad (\mathbf{x}, t) \in \Omega \times [0, t_{max}] \quad (9)$$

$$\nabla \cdot \mathbf{v}(\mathbf{x}, t) = 0, \quad (\mathbf{x}, t) \in \Omega \times [0, t_{max}] \quad (10)$$

$$\nabla^2\boldsymbol{\varphi}(\mathbf{x}, t) = \nabla \cdot (\mathbf{v}(\mathbf{x}, t) \times \mathbf{e}_B), \quad (\mathbf{x}, t) \in \Omega \times [0, t_{max}] \quad (11)$$

$$\theta(\mathbf{x}, 0) = \theta_i(\mathbf{x}), \quad \mathbf{v}(\mathbf{x}, 0) = \mathbf{v}_i(\mathbf{x}), \quad \mathbf{x} \in \Omega \quad (12)$$

$$\mathbf{v}(\mathbf{x}, t) = \mathbf{0}, \quad (\mathbf{x}, t) \in \Gamma \times [0, t_{max}] \quad (13)$$

$$\theta(\mathbf{x}, t) = \theta_g, \quad (\mathbf{x}, t) \in \Gamma_g \times [0, t_{max}] \quad (14)$$

$$\frac{\partial\theta}{\partial n}(\mathbf{x}, t) = q_1(\mathbf{x}, t), \quad (\mathbf{x}, t) \in \Gamma_{h1} \times [0, t_{max}] \quad (15)$$

$$\frac{\partial\theta}{\partial n}(\mathbf{x}, t) = q_o(\mathbf{x}, t), \quad (\mathbf{x}, t) \in \Gamma_{h0} \times [0, t_{max}] \quad (16)$$

$$\frac{\partial\boldsymbol{\varphi}}{\partial n}(\mathbf{x}, t) = 0, \quad (\mathbf{x}, t) \in \Gamma \times [0, t_{max}] \quad (17)$$

The objective is to calculate the unknown heat flux  $q_o(\mathbf{x}, t)$ ,  $(\mathbf{x}, t) \in \Gamma_{h0} \times [0, t_{max}]$  given Eqs. (4–5) and some additional temperature data. In this work, it is assumed that the temperature field is known in  $\Gamma_I \subset \Gamma_{h1}$ , i.e.

$$\theta(\mathbf{x}, t) = \theta_m(\mathbf{x}, t), \quad (\mathbf{x}, t) \in \Gamma_I \times [0, t_{max}], \quad (18)$$

The *overspecified* thermal boundary conditions on  $\Gamma_I$  are used to define an *ill-posed inverse problem* that can be solved to calculate  $q_o$  on  $\Gamma_{h0}$ . Once  $q_o$  is computed, a direct magneto-convection problem can be solved for the calculation of the temperature, velocity and electric field potential for each  $(\mathbf{x}, t) \in \Omega \times [0, t_{max}]$ .

In this work, it is assumed that a solution to the inverse problem exists in the sense of Tikhonov [19]. A *quasi-solution*  $\bar{q}_o(\mathbf{x}, t) \in L_2(\Gamma_{h0} \times [0, t_{max}])$  is needed such that  $J(\bar{q}_o) \leq J(q_o)$ ,  $\forall q_o \in L_2(\Gamma_{h0} \times [0, t_{max}])$ , where:

$$\begin{aligned} J(q_o) &= \frac{1}{2} \|\theta(\mathbf{x}, t; q_o) - \theta_m(\mathbf{x}, t)\|_{L_2(\Gamma_I \times [0, t_{max}])}^2 \\ &= \frac{1}{2} \int_0^{t_{max}} \int_{\Gamma_I} [\theta(\mathbf{x}, t; q_o) - \theta_m(\mathbf{x}, t)]^2 d\Gamma dt. \quad (19) \end{aligned}$$

In Eq. (19),  $\theta(\mathbf{x}, t; q_o)$  is defined as the solution of a direct magneto-convection problem with thermal boundary conditions given by Eqs. (4) and (5) and with  $q_o(\mathbf{x}, t)$  applied on  $\Gamma_{h0}$ . The direct problem that defines  $\theta$ ,  $\mathbf{v}$  and  $\boldsymbol{\varphi}$  is shown in Box I.

To solve the above optimization problem, one needs to calculate the gradient  $J'(q_o(\mathbf{x}, t))$  of  $J(q_o)$ . Introducing the directional derivative  $D_{\Delta q_o} J(q_o) \equiv (J'(q_o), \Delta q_o)_{L_2(\Gamma_{h0} \times [0, t_{max}])}$  and using Eq. (19), one can write the following:

$$\begin{aligned} D_{\Delta q_o} J(q_o) &\equiv (J'(q_o), \Delta q_o)_{L_2(\Gamma_{h0} \times [0, t_{max}])} \\ &= (\theta(\mathbf{x}, t; q_o) - \theta_m(\mathbf{x}, t), \Theta(\mathbf{x}, t; q_o, \Delta q_o))_{L_2(\Gamma_I \times [0, t_{max}])}, \quad (20) \end{aligned}$$

where the sensitivity fields  $\Theta$ ,  $\mathbf{V}$  and  $\Phi$ , are defined as the linear in  $\Delta q_o$  parts of  $\theta(\mathbf{x}, t; q_o + \Delta q_o)$ ,  $\mathbf{v}(\mathbf{x}, t; q_o + \Delta q_o)$  and  $\boldsymbol{\varphi}(\mathbf{x}, t; q_o + \Delta q_o)$ , respectively, calculated at  $q_o$ .

Based on Eq. (20), the calculation of the gradient  $J'(q_o)$  requires the evaluation of the adjoint to the sensitivity of the temperature operator. The definition of the sensitivity problem is given in Box II followed by the corresponding adjoint problem in Box III.

The Eqs. of Box II are derived by taking the directional derivatives of the governing equations of Box I, in the direction of  $\Delta q_o$  and calculated at the direct fields  $\theta(\mathbf{x}, t; q_o)$ ,  $\mathbf{v}(\mathbf{x}, t; q_o)$  and  $\boldsymbol{\varphi}(\mathbf{x}, t; q_o)$  corresponding to the boundary flux  $q_o$ . The solution of the *linear sensitivity magneto-convection problem* of Box II can be used to evaluate the fields  $\Theta(\mathbf{x}, t; q_o, \Delta q_o)$ ,  $\mathbf{V}(\mathbf{x}, t; q_o, \Delta q_o)$  and  $\Phi(\mathbf{x}, t; q_o, \Delta q_o)$ .

After some lengthy calculations [11], the equations of Box III can be derived to define the adjoint fields  $\psi$ ,  $\phi$  and  $\eta$ . With this definition of the *adjoint magneto-convection problem*, it can be shown that  $J'(q_o^k)$  is given as:

$$J'(q_o^k) = \psi(\mathbf{x}, t; q_o^k) \quad \text{for } (\mathbf{x}, t) \in \Gamma_{h0} \times [0, t_{max}] \quad (21)$$

## NUMERICAL IMPLEMENTATION

With the analytical expression for the exact gradient of Eq. (21), any of the standard functional minimization techniques can be used for solving the above defined optimization problem.

Here, the nonlinear conjugate gradient method (NCG) [10;14] is used to minimize the cost functional  $J(q_o)$ . The Polak-Ribière version of the nonlinear CG algorithm is adopted and the optimal step size corresponding to a quadratic approximation of the objective function is used.

### Box II

SENSITIVITY PROBLEM TO DEFINE  $\Theta(\mathbf{x}, t; q_o, \Delta q_o)$ ,  
 $\mathbf{V}(\mathbf{x}, t; q_o, \Delta q_o)$  AND  $\Phi(\mathbf{x}, t; q_o, \Delta q_o)$

$$\frac{\partial \Theta(\mathbf{x}, t)}{\partial t} + \mathbf{v}(\mathbf{x}, t) \cdot \nabla \Theta(\mathbf{x}, t) + \mathbf{V}(\mathbf{x}, t) \cdot \nabla \theta(\mathbf{x}, t) = \nabla^2 \Theta(\mathbf{x}, t), \quad (\mathbf{x}, t) \in \Omega \times [0, t_{max}] \quad (22)$$

$$\begin{aligned} \frac{\partial \mathbf{V}(\mathbf{x}, t)}{\partial t} + (\nabla \mathbf{V}(\mathbf{x}, t)) \mathbf{v}(\mathbf{x}, t) + (\nabla \mathbf{v}(\mathbf{x}, t)) \mathbf{V}(\mathbf{x}, t) = \nabla \cdot \boldsymbol{\Sigma}(\mathbf{x}, t) \\ - PrRa\Theta(\mathbf{x}, t)\mathbf{e}_g + Ha^2 Pr[-\nabla \Phi(\mathbf{x}, t) + \mathbf{V}(\mathbf{x}, t) \times \mathbf{e}_B] \times \mathbf{e}_B, \end{aligned} \quad (\mathbf{x}, t) \in \Omega \times [0, t_{max}] \quad (23)$$

$$\boldsymbol{\Sigma}(\mathbf{x}, t) = -\Pi(\mathbf{x}, t)\mathbf{I} + Pr[\nabla \mathbf{V}(\mathbf{x}, t) + (\nabla \mathbf{V}(\mathbf{x}, t))^T], \quad (\mathbf{x}, t) \in \Omega \times [0, t_{max}] \quad (24)$$

$$\nabla \cdot \mathbf{V}(\mathbf{x}, t) = 0, \quad (\mathbf{x}, t) \in \Omega \times [0, t_{max}] \quad (25)$$

$$\nabla^2 \Phi(\mathbf{x}, t) = \nabla \cdot (\mathbf{V}(\mathbf{x}, t) \times \mathbf{e}_B), \quad (\mathbf{x}, t) \in \Omega \times [0, t_{max}] \quad (26)$$

$$\Theta(\mathbf{x}, 0) = 0, \quad \mathbf{x} \in \Omega, \quad \mathbf{V}(\mathbf{x}, 0) = \mathbf{0}, \quad \mathbf{x} \in \Omega \quad (27)$$

$$\mathbf{V}(\mathbf{x}, t) = \mathbf{0}, \quad (\mathbf{x}, t) \in \Gamma \times [0, t_{max}] \quad (28)$$

$$\Theta(\mathbf{x}, t) = 0, \quad (\mathbf{x}, t) \in \Gamma_g \times [0, t_{max}] \quad (29)$$

$$\frac{\partial \Theta}{\partial n}(\mathbf{x}, t) = 0, \quad (\mathbf{x}, t) \in \Gamma_{h1} \times [0, t_{max}] \quad (30)$$

$$\frac{\partial \Theta}{\partial n}(\mathbf{x}, t) = \Delta q_o(\mathbf{x}, t), \quad (\mathbf{x}, t) \in \Gamma_{ho} \times [0, t_{max}] \quad (31)$$

$$\frac{\partial \Phi}{\partial n}(\mathbf{x}, t) = 0, \quad (\mathbf{x}, t) \in \Gamma \times [0, t_{max}] \quad (32)$$

The stabilized FEM using an equal-order velocity-pressure interpolation method [17;18] is adopted here for the fluid flow sub-problem. This method achieves stabilization by adding two terms to the standard Galerkin formulation of the problem. The first term is the well-known SUPG (streamline-upwind/Petrov-Galerkin) term, whereas the second PSPG term (pressure stabilizing/Petrov-Galerkin) was introduced in [17;18] to accommodate equal-order-interpolation velocity-pressure elements. The above formulation for the fluid flow sub-problem is combined with the SUPG formulation for the heat equation and a classical Galerkin formulation for the electric potential equation. The numerical methodology developed for the direct problem has been tested extensively and is found to compare well with other implementations [3]. The time integration scheme for the sensitivity and adjoint equations is the same as that used in the direct analysis. Due to the *backward in time* solution of the adjoint problem, the entire history of the solution of the direct problem needs to be stored [21].

The gradient of the cost functional in the nonlinear optimization problem is computed in this paper using a ‘differentiate-then-

discretize’ approach, i.e., the sensitivities and adjoint fields are first defined in the function space framework and then are discretized. In general, the gradient of the cost functional computed using this technique differs from that obtained with the ‘discretize-then-differentiate’ approach (see e.g. [4]), in which the discretized state equations are differentiated and adjoint fields are computed from those derivatives.

### Box III

ADJOINT PROBLEM TO DEFINE  $\psi(\mathbf{x}, t; q_o)$ ,  $\phi(\mathbf{x}, t; q_o)$  AND  $\eta(\mathbf{x}, t; q_o)$

$$\frac{\partial \psi(\mathbf{x}, t)}{\partial t} + \mathbf{v}(\mathbf{x}, t) \cdot \nabla \psi(\mathbf{x}, t) = -\nabla^2 \psi(\mathbf{x}, t) + \dot{\phi}(\mathbf{x}, t) \cdot \mathbf{e}_g, \quad (\mathbf{x}, t) \in \Omega \times [0, t_{max}] \quad (33)$$

$$\begin{aligned} \frac{\partial \phi(\mathbf{x}, t)}{\partial t} + (\nabla \phi(\mathbf{x}, t)) \mathbf{v}(\mathbf{x}, t) - (\nabla \mathbf{v}(\mathbf{x}, t))^T \phi(\mathbf{x}, t) = -\nabla \cdot \boldsymbol{\zeta}(\mathbf{x}, t) \\ + PrRa\psi(\mathbf{x}, t)\nabla \theta(\mathbf{x}, t) - Ha^2 Pr[\mathbf{e}_B(\dot{\phi}(\mathbf{x}, t) \cdot \mathbf{e}_B) - \dot{\phi}(\mathbf{x}, t)] \\ + Ha^2 Pr[\nabla \eta(\mathbf{x}, t) \times \mathbf{e}_B], \end{aligned} \quad (\mathbf{x}, t) \in \Omega \times [0, t_{max}] \quad (34)$$

$$\boldsymbol{\zeta}(\mathbf{x}, t) = -\pi(\mathbf{x}, t)\mathbf{I} + Pr[\nabla \phi(\mathbf{x}, t) + (\nabla \phi(\mathbf{x}, t))^T], \quad (\mathbf{x}, t) \in \Omega \times [0, t_{max}] \quad (35)$$

$$\nabla \cdot \phi(\mathbf{x}, t) = 0, \quad (\mathbf{x}, t) \in \Omega \times [0, t_{max}] \quad (36)$$

$$\nabla^2 \eta(\mathbf{x}, t) = \nabla \cdot (\phi(\mathbf{x}, t) \times \mathbf{e}_B), \quad (\mathbf{x}, t) \in \Omega \times [0, t_{max}] \quad (37)$$

$$\psi(\mathbf{x}, t_{max}) = 0, \quad \mathbf{x} \in \Omega, \quad \phi(\mathbf{x}, t_{max}) = \mathbf{0}, \quad \mathbf{x} \in \Omega \quad (38)$$

$$\dot{\phi}(\mathbf{x}, t) = \mathbf{0}, \quad (\mathbf{x}, t) \in \Gamma \times [0, t_{max}] \quad (39)$$

$$\psi(\mathbf{x}, t) = 0, \quad (\mathbf{x}, t) \in \Gamma_g \times [0, t_{max}] \quad (40)$$

$$\frac{\partial \psi}{\partial n}(\mathbf{x}, t) = 0, \quad (\mathbf{x}, t) \in (\Gamma_h - \Gamma) \times [0, t_{max}] \quad (41)$$

$$\frac{\partial \psi}{\partial n}(\mathbf{x}, t) = \theta(\mathbf{x}, t) - \theta_m(\mathbf{x}, t), \quad (\mathbf{x}, t) \in \Gamma_l \times [0, t_{max}] \quad (42)$$

$$\frac{\partial \eta}{\partial n}(\mathbf{x}, t) = 0, \quad (\mathbf{x}, t) \in \Gamma \times [0, t_{max}] \quad (43)$$

### $H^1$ REGULARIZATION

To deal with the ill-posedness introduced in problems with random errors in the data  $\theta_m$ , a  $H^1$  type regularization is considered. In particular, the cost functional is modified as follows:

$$\begin{aligned} J(q_o) = \frac{1}{2} \|\theta(\mathbf{x}, t; q_o) - \theta_m(\mathbf{x}, t)\|_{L_2(\Gamma_l \times [0, t_{max}])}^2 \\ + \frac{\gamma}{2} \|q_o\|_{L_2(\Gamma_{ho} \times [0, t_{max}])}^2 \\ + \frac{\gamma}{2} \|\nabla q_o\|_{L_2(\Gamma_{ho} \times [0, t_{max}])}^2, \end{aligned} \quad (44)$$

where  $\gamma \in \mathfrak{R}^+$  is an appropriate regularization parameter [2;5].

The directional derivative of the cost functional becomes:

$$D_{\Delta q_o} J(q_o) \equiv (\psi(\mathbf{x}, t; q_o), \Delta q_o)_{L_2(\Gamma_{ho} \times [0, t_{max}])}$$

$$\begin{aligned}
& + \gamma(q_o(\mathbf{x}, t), \Delta q_o)_{L_2(\Gamma_{h0} \times [0, t_{max}])} \\
& + \gamma(\nabla q_o(\mathbf{x}, t), \nabla(\Delta q_o))_{L_2(\Gamma_{h0} \times [0, t_{max}])}. \quad (45)
\end{aligned}$$

Let us denote with  $z(\mathbf{x}, t)$  the solution to the following variational equation:

$$\begin{aligned}
(z(\mathbf{x}, t), w)_{L_2(\Gamma_{h0})} + (\nabla z(\mathbf{x}, t), \nabla w)_{L_2(\Gamma_{h0})} \\
= (\psi(\mathbf{x}, t; q_o), w)_{L_2(\Gamma_{h0})} \quad (46)
\end{aligned}$$

$\forall w \in H^1(\Gamma_{h0})$  and for  $t \in [0, t_{max}]$ . Setting  $w = \Delta q_o$ , the derivative of the cost functional can now be written as follows:

$$\begin{aligned}
D_{\Delta q_o} J(q_o) = (z(\mathbf{x}, t) + \gamma q_o(\mathbf{x}, t), \Delta q_o)_{L_2(\Gamma_{h0} \times [0, t_{max}])} \\
+ (\nabla z(\mathbf{x}, t) + \gamma \nabla q_o(\mathbf{x}, t), \nabla(\Delta q_o))_{L_2(\Gamma_{h0} \times [0, t_{max}])}. \quad (47)
\end{aligned}$$

The gradient of  $J(q_o)$  with respect to the scalar product  $(\cdot, \cdot)_Q \equiv (\cdot, \cdot)_{L_2(\Gamma_{h0} \times [0, t_{max}])} + (\nabla \cdot, \nabla \cdot)_{L_2(\Gamma_{h0} \times [0, t_{max}])}$  is therefore given by

$$J'(q_o) = z + \gamma q_o \quad (48)$$

Thus, to calculate the gradient of the cost functional in the case of regularization, the solution component  $\psi(\mathbf{x}, t; q_o)$  of the adjoint equations listed in Box III has to be first computed. An additional variational equation has to be solved on  $\Gamma_{h0}$ , in particular:

$$-\Delta z(\mathbf{x}, t) + z(\mathbf{x}, t) = \psi(\mathbf{x}, t; q_o) \quad (49)$$

In the solution of the above equation, Neumann boundary conditions are applied on  $\partial\Gamma_{h0}$  (boundary of  $\Gamma_{h0}$ ).

Note that, since the gradient of the objective functional is calculated with respect to the scalar product  $(\cdot, \cdot)_Q$ , the same scalar product/norm has to be used in the conjugate gradient algorithm (see Box IV).

## NUMERICAL EXAMPLE

Let us consider a two-dimensional square cavity filled with a fluid of Prandtl number equal to 0.01, a value characteristic of liquid metals and semiconductors [3]. The fluid is initially at a dimensionless homogeneous temperature  $\theta_i = 1.0$ . The top and bottom walls of the cavity are insulated (Fig. 2). The left wall ( $x = 0$ ) is maintained at a constant temperature of  $\theta_m = 0$  for times  $t > 0$  while a linear heat flux profile  $q_o(y, t) = 1 - t$  is applied on the right wall ( $x = 1.0$ ). The Rayleigh number of the system is 20000. The fluid contained in the cavity is subject to a magnetic field directed at an angle  $45^\circ$  to the x-axis. The Hartmann number corresponding to this field is 75. The solution of the

direct magneto-convection problem corresponding to the above data with a uniform  $20 \times 20$  mesh and  $\Delta t = 0.0025$  results in the heat flux history  $q_I(y, t)$  on the left wall (Fig. 3). The asymptotic estimate [3] for the Hartmann boundary layer thickness is as  $1/Ha \approx 0.01$ . Despite this fact, it was found through mesh-related studies that the  $20 \times 20$  mesh used here was sufficient to accurately capture the main flow field.

## Box IV

### THE NONLINEAR CONJUGATE GRADIENT ALGORITHM

Step I : Make an initial guess of  $q_o^0 \in H^1(\Gamma_{h0} \times [0, t_{max}])$ , calculate  $\nabla q_o^0$  and set  $k = 0$ .

Step II : Calculate the conjugate search direction  $p^k(\mathbf{x}, t)$ ,  $(\mathbf{x}, t) \in \Gamma_{h0} \times [0, t_{max}]$ :

1. Solve the coupled direct problem for  $\theta(\mathbf{x}, t; q_o^k)$ ,  $\mathbf{v}(\mathbf{x}, t; q_o^k)$  and  $\phi(\mathbf{x}, t; q_o^k)$ .
2. Evaluate  $J(q_o^k)$  from Eq. (44); If  $J(q_o^k) < \textit{tolerance}$ , set  $\bar{q}_o = q_o^k$  and stop.
3. Solve the coupled adjoint problem backwards in time for  $\psi(\mathbf{x}, t; q_o^k)$ ,  $\Phi(\mathbf{x}, t; q_o^k)$  and  $\eta(\mathbf{x}, t; q_o^k)$ .
4. Solve Eq. (49) for  $z(\mathbf{x}, t; q_o^k)$  for  $(\mathbf{x}, t) \in \Gamma_{h0} \times [0, t_{max}]$  and calculate  $\nabla z(\mathbf{x}, t; q_o^k)$ .
5. Set  $J'(q_o^k) = z(\mathbf{x}, t; q_o^k) + \gamma q_o^k$  for  $(\mathbf{x}, t) \in \Gamma_{h0} \times [0, t_{max}]$  and calculate  $\nabla J'(q_o^k)$ .
6. Set  $\gamma^k = 0$ , if  $k = 0$ ; otherwise:  

$$\gamma^k = \frac{(J'(q_o^k), J'(q_o^k) - J'(q_o^{k-1}))_Q}{\|J'(q_o^{k-1})\|_Q^2}.$$
7. Define  $p^k(\mathbf{x}, t)$ : If  $k = 0$ ,  $p^0 = -J'(q_o^k)$ ,  $\nabla p^0 = -\nabla J'(q_o^k)$  ;  
Otherwise: 
$$p^k = -J'(q_o^k) + \gamma^k p^{k-1};$$

$$\nabla p^k = -\nabla J'(q_o^k) + \gamma^k \nabla p^{k-1}.$$

Step III : Calculate the optimal step size  $\alpha^k$ :

1. Solve the coupled sensitivity problem for  $\Theta(\mathbf{x}, t; q_o^k, p^k)$ ,  $\mathbf{V}(\mathbf{x}, t; q_o^k, p^k)$  and  $\Phi(\mathbf{x}, t; q_o^k, p^k)$ .
2. Calculate  $\alpha^k$ :  

$$\alpha^k = \frac{-[(J'(q_o^k), p^k)_{L_2(\Gamma_{h0} \times [0, t_{max}])} + \gamma(q_o^k, p^k)_Q]}{[\|\Theta(\mathbf{x}, t; q_o^k, p^k)\|_{L_2(\Gamma_{h0} \times [0, t_{max}])}^2 + \gamma\|p^k\|_Q^2]}.$$

Step IV : Update  $q_o^{k+1}(\mathbf{x}, t) = q_o^k(\mathbf{x}, t) + \alpha^k p^k(\mathbf{x}, t)$ ;  
 $\nabla q_o^{k+1}(\mathbf{x}, t) = \nabla q_o^k(\mathbf{x}, t) + \alpha^k \nabla p^k(\mathbf{x}, t)$ ,  $(\mathbf{x}, t) \in \Gamma_{h0} \times [0, t_{max}]$ .

Step V : Set  $k = k + 1$  and return to Step II.

The following inverse problem is posed:

*With the bottom and top cavity walls insulated and a known heat flux history  $q_I(y, t)$ ,  $t \in [0, 1]$  applied at  $x = 0$ , find the heat flux history,  $q_o(y, t)$ , at the right side wall, in order to maintain a temperature  $\theta_m(y, t) \equiv 0$ ,  $t \in [0, 1]$ , at  $x = 0$  and  $y \in [0, 1]$ .*

Note that both temperature and flux are prescribed on the left vertical wall, whereas no boundary conditions are available at  $x = 1$ . The exact solution is  $\bar{q}_o(y, t) = 1 - t$ .

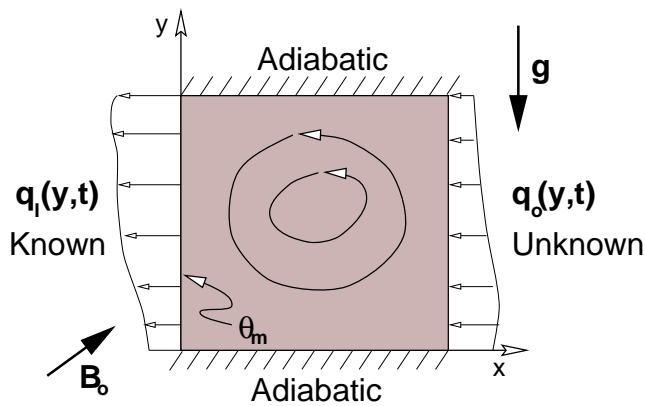


Figure 2. THE EXAMPLE PROBLEM.

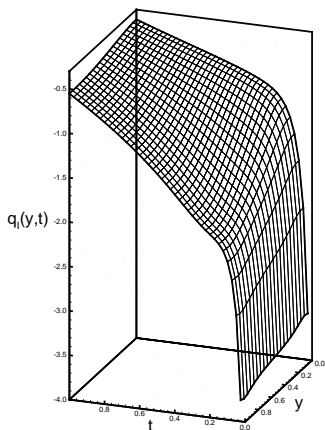


Figure 3. GIVEN HEAT FLUX HISTORY  $q_l(y,t)$  ON THE LEFT VERTICAL WALL OF THE CAVITY.

$20 \times 20$  bilinear uniform rectangular elements are used in the analysis of the direct, sensitivity and adjoint problems, with time step  $\Delta t = 0.0025$  for all of them. The maximum time is taken as  $t_{max} = 1$ . The total number of time steps for the solution of each direct, sensitivity and adjoint problems in one global NCG iteration is 400.

The initial guess for the heat flux is taken as  $q_o^0 \equiv 0$ . The calculated solution at three intermediate iteration steps without any regularization (and exact temperature input data) is shown in Fig. 4. Figure 5(a) shows the optimal heat flux solution (corresponding to 35 iterations) for a tolerance of  $\epsilon = 3.5 \times 10^{-9}$ . Figure 5(b) shows the monotonic reduction of the cost functional  $J(q_o^k)$  with the number of NCG iterations  $k$ . The  $L_2$  norm  $\|J'(q_o^k)\|$  of the gradient of the cost functional is also shown in Fig. 5(b). It is defined as  $\|J'(q_o^k)\| \equiv (\psi(\mathbf{x}, t; q_o^k), \psi(\mathbf{x}, t; q_o^k))_{L_2(\Gamma_{10} \times [0, t_{max}])}^{1/2}$ . Note that the norm  $\|J'(q_o^k)\|$  decreases with the number of iterations, but not monotonically. Similar behavior has been observed in related optimization processes [21].

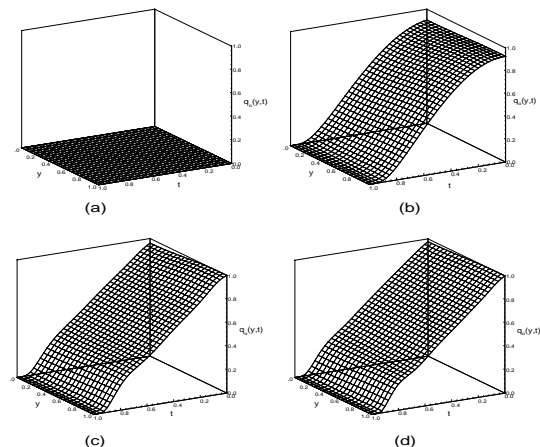


Figure 4. INITIAL GUESS  $q_o^0 = 0$  AND INTERMEDIATE FLUXES  $q_o^k(y,t)$  AT ITERATIONS 1, 10, 20 (CASE I,  $q_o^0 = 0$ , EXACT DATA  $\theta_m$ , NO REGULARIZATION).

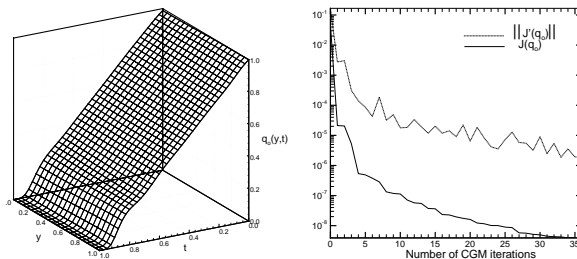


Figure 5. (a) THE OPTIMAL HEAT FLUX DISTRIBUTION CALCULATED AT THE 35<sup>th</sup> NCG ITERATION (b) VARIATION OF THE COST FUNCTION  $J(q_o^k)$  AND OF THE NORM OF THE GRADIENT  $\|J'(q_o^k)\|$  WITH NCG ITERATION COUNTER  $k$  (CASE I,  $q_o^0 = 0$ , EXACT DATA  $\theta_m$ , NO REGULARIZATION).

To study the effects of the initial guess heat flux on the convergence behavior of the proposed NCG algorithm, the above example without regularization was repeated with a different starting point. In particular, an initial guess of  $q_o^0 = 1 - t^4$  was used to start the NCG iterations. Figure 6 shows the variation of the calculated heat flux profiles for some intermediate iterations. Figure 7(a) shows the optimal heat flux solution calculated after 60 NCG iterations with the same tolerance as in the earlier example. Note the prominent deviation of the above flux distribution from the exact solution  $\bar{q}_o \equiv 1 - t$  at times close to  $t = t_{max}$ . This is mainly due to the fact that the solution  $q_o^k(y, t_{max})$  at all iterations  $k$  is constrained such that  $q_o^k(y, t_{max}) = q_o^0(y, t_{max})$  and  $\partial q_o^k(y, t_{max}) / \partial t = \partial q_o^0(y, t_{max}) / \partial t$ , for all  $y \in [0, 1]$ . Indeed, from the equations of Box III at time  $t_{max}$ , one can show that  $\psi(1, y, t_{max}) = 0$  and  $\partial \psi(1, y, t_{max}) / \partial t = 0$ . These equations together with the update formula in the Step IV of Box IV, lead to the above constraints on  $q_o^k(y, t_{max})$  and  $\partial q_o^k(y, t_{max}) / \partial t$ . As can be seen from Fig. 6, the NCG algorithm approaches the exact solution  $\bar{q}_o = 1 - t$  with

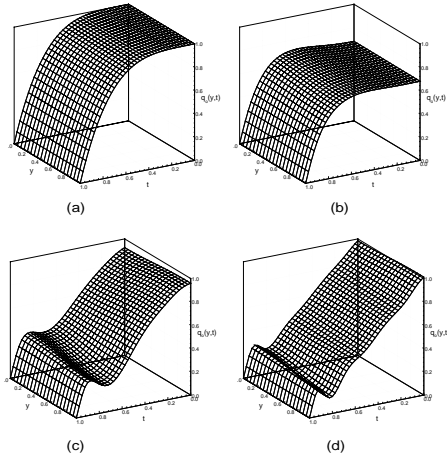


Figure 6. INITIAL AND INTERMEDIATE FLUXES  $q_o^k(y,t)$  AT ITERATIONS 1, 5, 20 (CASE II,  $q_o^0 = 1 - t^4$ , EXACT DATA  $\theta_m$ , NO REGULARIZATION).

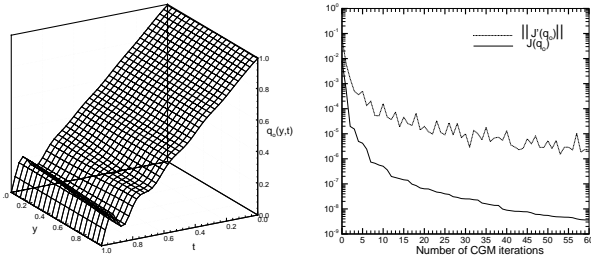


Figure 7. (a) THE OPTIMAL HEAT FLUX DISTRIBUTION CALCULATED AT THE 60<sup>th</sup> NCG ITERATION (b) VARIATION OF THE COST FUNCTIONAL  $J(q_o^k)$  AND OF THE NORM OF THE GRADIENT  $\|J'(q_o^k)\|$  WITH NCG ITERATION COUNTER  $k$  (CASE II,  $q_o^0 = 1 - t^4$ , EXACT DATA  $\theta_m$ , NO REGULARIZATION).

the constraint that  $q_o^k(y, t_{max})$  and  $\partial q_o^k(y, t_{max})/\partial t$  retain the values of  $q_o^0(y, t_{max})$  and  $\partial q_o^0(y, t_{max})/\partial t$ , respectively (Fig. 6). The importance of the end conditions of the adjoint problem is reviewed in [1].

Figure 7(b) shows the variation of the cost functional  $J(q_o^k)$  and the norm of the gradient  $\|J'(q_o^k)\|$  with the NCG iteration counter  $k$ . The prominent effect of  $q_o^k$  on the convergence of the NCG is apparent (compare Figs. 5(b) and 7(b)).

We next study the effects of large fluctuating temperature measurement errors on the convergence and stability of the proposed methodology. The objective of the inverse problem is now defined as the calculation of the heat flux history  $q_o(y,t)$  on the right side wall using a known heat flux history  $q_I(y,t)$  (see Fig. 3) and a fluctuating temperature data  $\theta(y,t) \equiv \theta_m(y,t)$  provided on the left hand side wall for  $t \in [0, 1]$ . The top and bottom cavity walls are insulated as before. The fluctuating temperature data is taken as  $\tilde{\theta}_m(y,t) = \theta_m(y,t) + \varepsilon \omega_n$ , where

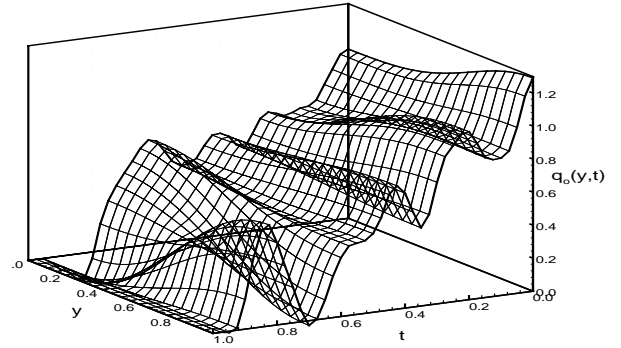


Figure 8. THE CALCULATED HEAT FLUX SOLUTION AT THE 30<sup>th</sup> ITERATION (CASE III,  $q_o^0 = 0$ , INEXACT DATA  $\theta_m$ , NO REGULARIZATION).

$\theta_m(y,t) \equiv 0$ ,  $\varepsilon = 0.05$  and  $\omega_n$  are uniformly distributed random numbers in the interval  $[-1, 1]$ . In the first few iterations, the NCG algorithm reveals the basic structural features of the unknown solution and the calculated solution at around the 3rd NCG iteration is quite close to the actual exact solution with exact data (i.e. to  $\bar{q}_o = 1 - t$ ). However, after around 7 or 8 NCG iterations, the computations show that an oscillating nature of the solution develops gradually and a “build-up” of the amplitude of oscillations unfolds slowly. The calculated solution at the end of 30 NCG iterations is shown in Fig. 8. Clearly the solution obtained is unacceptable. This implies that in problems involving sufficiently large amplitude noise in the input data, the “viscous” properties (i.e. slow convergence of the method while nearing the minima, see chapter 6 in [1]) of the CG method are not sufficient to damp oscillations in the solution. Figure 9 shows the calculated flux using the  $H^1$  regularized formulation. The regularization parameter  $\gamma$  is set to be  $2 \times 10^{-4}$ . As can be clearly seen the obtained solution is much smoother and has no significant oscillations.

## CONCLUSIONS AND FURTHER APPLICATIONS

Functional optimization methods were presented for the design of thermo-magnetically driven flows. The work presented here is currently being extended to the solution of inverse problems in thermal transport systems with simultaneous coupled momentum, heat and mass transfer mechanisms as well as electromagnetics. We mainly address inverse problems with over-specified boundary conditions in one part of the boundary and unknown thermal conditions in another part of the boundary. Our particular interest and motivation for examining such coupled transport systems arise from the design of solidification processes that lead to desired microstructures in the final product.

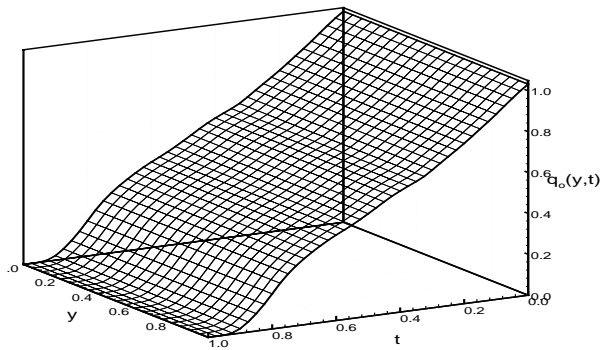


Figure 9. THE CALCULATED HEAT FLUX SOLUTION AT THE 30<sup>th</sup> ITERATION (CASE IV,  $q_0^0 = 0$ , INEXACT DATA  $\theta_m$ ,  $H^1$  REGULARIZATION).

In particular, we address the calculation of the mold/furnace heat flux conditions such that a desired solidification state (growth rate at which solidification occurs and temperature field near the solid/melt interface) is achieved at the freezing interface. Changes in growth rate and thermal gradient at the freezing interface are known to alter the relative importance of thermal/mass transport and interfacial energy effects, and the magnitude of this partitioning of available driving forces dictates the formation of specific microstructures [8].

## ACKNOWLEDGMENT

The results presented in this paper were obtained in the course of research sponsored by ALCOA. The authors also gratefully acknowledge the computing support provided by the Cornell Theory Center.

## REFERENCES

[1] Alifanov, O.M., *Inverse Heat Transfer Problems*, (Springer-Verlag, Berlin, 1994).  
 [2] Banks, H.T. and K. Kunisch, *Estimation Techniques for Distributed Parameter Systems*, (Birkhäuser, Boston; Basel; Berlin, 1989).  
 [3] Ben Hadid, H., D. Henry and S. Kaddeche, Numerical study of convection in the horizontal Bridgman configuration under the action of a constant magnetic field. Part 1. Two-dimensional flow, *J. Fluid Mech.* 333 (1997) 23–56.  
 [4] Berggren, M., Numerical solution of a flow-control problem: Vorticity reduction by dynamic boundary action, *SIAM J. Sci. Comput.* 19 (1998) 829–860.  
 [5] Engl, H. W., M. Hanke and A. Neubauer, *Regularization of Inverse Problems*, (Kluwer Academic Publishers, Boston, 1996).

[6] Gunzburger, M.D., L. Hou and T. Svobodny, Heating and cooling control of temperature distributions along boundaries of flow domains, *J. Math. Syst. Estim. Control* 3(2) (1993) 147–172.  
 [7] Gunzburger, M.D. and H. C. Lee, Analysis, approximation, and computation of a coupled solid/fluid temperature control problem, *Comput. Methods Appl. Mech. Engrg.* 118 (1994) 133–152.  
 [8] Kurz, W. and D. J. Fisher, *Fundamentals of Solidification*, (Trans Tech Publications Ltd, Switzerland, 1989).  
 [9] Lielausis, O., Liquid metal in a strong magnetic field, in: J. Lielpeteris and R. Moreau, eds., *Proceedings Liquid Metal Magnetohydrodynamics* (Riga, USSR, 1990) 3–12.  
 [10] Luenberger, D.G., *Optimization by Vector Space Methods*, (Wiley-Interscience, New York, 1990).  
 [11] Marchuk, G.I., *Adjoint Equations and Analysis of Complex Models*, (Kluwer Academic Publishers, Boston, 1995).  
 [12] Moreau, R., *Magnetohydrodynamics*, (Kluwer Academic Publishers, Boston, 1990).  
 [13] Moutsoglou, A., An inverse convection problem, *J. Heat Trans., ASME* 111 (1989) 37–43.  
 [14] Nocedal, J. and S. J. Wright, *Numerical Optimization*, (Springer Verlag, New York, 1999).  
 [15] Sampath, R. and N. Zabaras, Inverse thermal design of solidification processes in the presence of a strong external magnetic field, *Int. J. Numer. Methods Engrg.*, in review.  
 [16] Series, R.W. and D. T. J. Hurle, The use of magnetic fields in semiconductor crystal growth, *J. Cryst. Growth* 113 (1991) 305–328.  
 [17] Tezduyar, T. E., Stabilized finite element formulations for incompressible flow computations, *Adv. Appl. Mech.* 28 (1992) 1–43.  
 [18] Tezduyar, T.E., S. Mittal, S. E. Ray and R. Shih, Incompressible flow computations with stabilized bilinear and linear equal-order-interpolation velocity-pressure elements, *Comput. Methods Appl. Mech. Engrg.* 95 (1992) 221–242.  
 [19] Tikhonov, A.N., *Solutions of ill-posed problems*, (Halsted Press, Washington; inston; New York, 1977).  
 [20] Yang, G.Z. and N. Zabaras, The adjoint method for an inverse design problem in the directional solidification of binary alloys, *J. Comput. Phys.* 140 (1998) 432–452.  
 [21] Zabaras, N. and G.Z. Yang, A functional optimization formulation and implementation of an inverse natural convection problem, *Comput. Methods Appl. Mech. Engrg.* 144 (1997) 245–274.  
 [22] Zabaras, N. Adjoint methods for inverse free convection problems with applications to solidification processes, in: J. Borggaard, E. Cliff, S. Schreck and J. Burns, eds., *Computational Methods for Optimal Design and Control*, Birkhauser Series in Progress in Systems and Control Theory, Birkhauser, 1998, 391–426.